Biogenesis of the T1−S1 Linker of Voltage-Gated K^+ Channels†

LiWei Tu, Jing Wang, and Carol Deutsch*

Department of Physiology, University of Pennsylvania, Philadelpha, Pennsylvania 19104-6085

Received February 14, 2007; Revised Manuscript Received April 17, 2007

ABSTRACT: In the model derived from the crystal structure of Kv1.2, a six-transmembrane voltage-gated potassium channel, the linker between a cytosolic tetramerization domain, T1, and the first transmembrane segment, S1, is projected radially outward from the channel's central axis. This T1−S1 linker was modeled as two polyglycine helices to accommodate the residues between T1 and S1 [Long et al. (2005) *Science 309*, 897−903]; however, the structure of this linker is not known. Here, we investigate whether a compact secondary structure of the T1−S1 linker exists at an early stage of Kv channel biogenesis. We have used a mass-tagging accessibility assay to report the biogenesis of secondary structure for three consecutive regions of Kv1.3, a highly homologous isoform of Kv1.2. The three regions include the T1−S1 linker and its two flanking regions, α5 of the T1 domain and S1. Both α5 and S1 manifest compact structures (helical) inside the ribosomal exit tunnel, whereas the T1−S1 linker does not. Moreover, the location of the peptide in the tunnel influences compaction.

Voltage-gated K^+ (Kv)[1] channels are critical to the normal functioning of excitable and non-excitable cells (*1*, *2*). Defects in their biophysical properties, biogenesis, assembly, and/or trafficking underlie channelopathies and can be lethal. It is therefore important to understand the events leading to proper folding of Kv channel proteins. Kv channels are composed of four subunits. Each subunit contains six transmembrane segments, S1−S6, a pore region comprised of S5, S6, and a pore loop, and an N-terminal cytosolic domain known as T1. The isolated T1 domain has been crystallized (*3*−*5*), and in the full-length channel, this domain resides directly under the pore as a hanging gondola, a distance of ∼20 Å (*6*−*8*). Recently, a mature mammalian Kv channel, Kv1.2, was crystallized and diffracted to 2.9 Å resolution (*7*). Although this structure has advanced our understanding of the pore region and voltage-sensing domain, it is less definitive regarding other regions, including cytosolic linkers. In Kv1.2, the linker connecting the T1 domain to the first transmembrane segment, S1, referred to as the T1−S1 linker, was projected radially outward from the channel's central axis to create a wide space between the T1 domain and the pore (Figure 1A). The T1−S1 linker appears to function as a spacer to maintain a separation between the transmembrane pore and intracellular regions of the channel. In the crystal structure, the resolution of S1 and the T1−S1 linker is very poor, and the T1−S1 linker was built as two polyglycine helices to accommodate the residues between T1 and S1. The structure of the T1−S1 linker is still unknown. If both S1 and the T1−S1 linker do form α-helices in the mature Kv channel, is this secondary structure manifest at early stages of Kv biogenesis? We do not know whether secondary structure is acquired while the nascent Kv peptide emerges from the ribosomal exit tunnel, nor the compartment in which structure is acquired, nor the chain length required for secondary structure formation.

Protein synthesis begins in the ribosome at the peptidyl transfer center (PTC) in the cleft between the small and large ribosome subunits. While still tethered to the PTC on one side of the large subunit, the nascent peptide is elongated, extending along a tunnel to the exit port on the other side of the large subunit. This tunnel is ∼100 Å long with a diameter of ≤10 Å at its narrowest and ∼20 Å at its widest point near the exit site (*9*−*12*), capable of accommodating the dimensions of an α-helix (*13*). Indeed, compact peptide structures, including an α-helix do form inside the ribosome (*14*−*20*) and could serve a signaling role (*21*).

To determine secondary structure formation inside the ribosomal exit tunnel, we used an all-extended molecular tape measure (*19*) and a mass-tagging cysteine accessibility assay (*17*, *19*). This assay involves pegylation, modification of a cysteine with polyethylene glycol maleimide (PEG-MAL; *22*). The cysteines are engineered, one at a time, at various positions along a nascent peptide. We have previously demonstrated that both the final extent and the rates of pegylation increase monotonically with distance from the PTC and that the emergent length of the modifiable cysteine reflects secondary structure of the nascent peptide (*19*). A cysteine buried inside the tunnel is relatively inaccessible compared to a cysteine that has emerged from the tunnel. Using this assay, we have shown that the S6 transmembrane segment and some regions of the cytosolic N-terminal T1 domain, in the nascent peptide in the monomer, have an α-helical conformation, similar to that in the crystal structure of the mature Kv1.2 (*17*, *19*). Both regions begin to form compact structures before they emerge completely from the ribosomal exit tunnel and while the peptide is still attached to the ribosome (*17*, *19*). This suggests that, at least for some Kv segments, analysis of early events in biogenesis may

† Supported by National Institutes of Health Grant GM 52302.

* Corresponding author. Phone: 215-898-8014. Fax: 215-573-5851. E-mail: cjd@mail.med.upenn.edu.

[1] Abbreviations: PTC: peptidyl transferase center; Kv: voltage-gated K^+; PEG-MAL: polyethylene glycol maleimide.

10.1021/bi700319f CCC: $37.00
Published on Web 06/13/2007

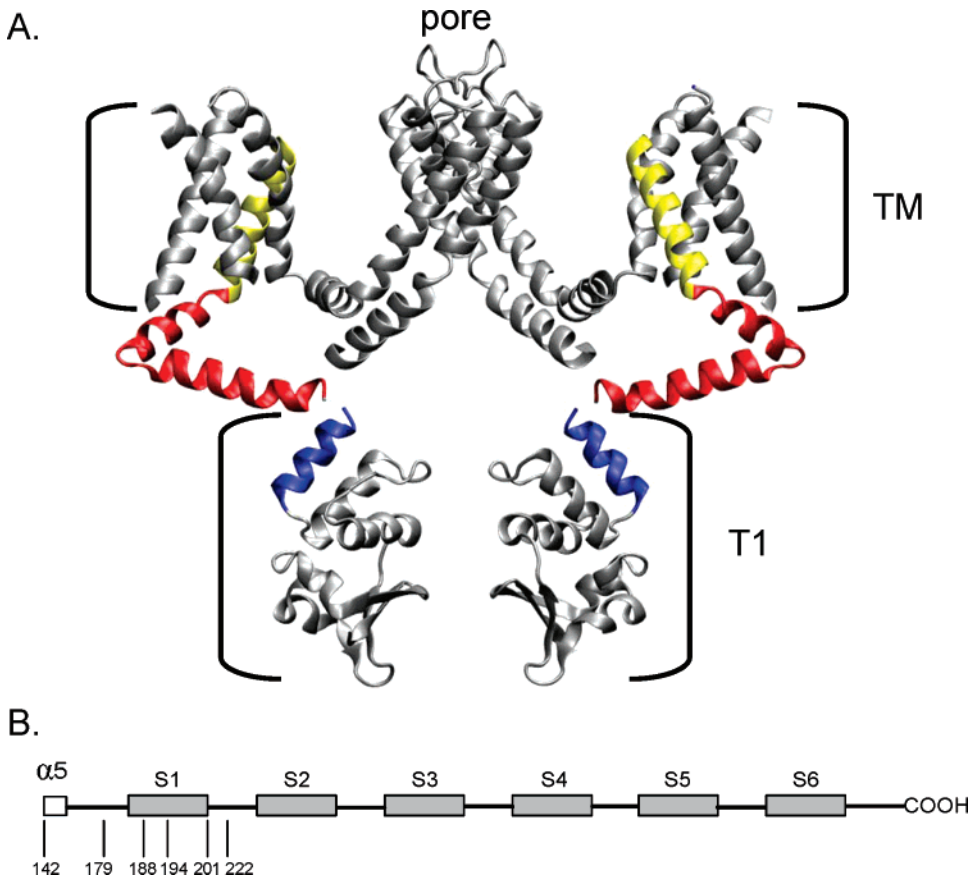

FIGURE 1: Kv region of investigation. (A) A ribbon representation of Kv1.2 was made in DS ViewerPro (http://www.accelrys.com) from Long et al. (*7*). Two subunits are shown. The T1−S1 linker, shown in red, is estimated to have 33 residues following the C-terminal end of the T1 domain. The S1 transmembrane segment is shown in yellow, and the α5 helix in the T1 domain is shown in blue. (B) Schematic drawing of ΔT1 Kv1.3. The gray boxes represent the six transmembrane segments (S1−S6), and the white box represents the α5 region. The numbers represent the restriction enzyme sites used in this study. The start site of ΔT1 Kv1.3 is 142.

faithfully reflect the final conformation in the mature Kv channel.

In this paper, we report on the biogenesis of secondary structure of three distinct regions of Kv1.3, namely, the α5 helix of the T1 domain, the T1−S1 linker, and the S1 transmembrane segment. We draw the following conclusions. First, the α5 helix manifests compact secondary structure in the nascent peptide before it emerges from the ribosomal exit tunnel. Second, the T1−S1 linker does not form a compact structure, regardless of its location inside the tunnel. Third, S1 compacts only when it is positioned in the last 20 Å of the tunnel, near the exit port.

MATERIALS AND METHODS

Constructs and In Vitro Translation. Standard methods of bacterial transformation, plasmid DNA preparation, and restriction enzyme analysis were used. The nucleotide sequences of all mutants were confirmed by automated cycle sequencing performed by the DNA Sequencing Facility at the School of Medicine on an ABI 377 sequencer using Big dye terminator chemistry (A0BI). pSP/(ΔT1)Kv1.3 was constructed by re-ligation of the *Hind*III/*Nco*I-digested, blunt-ended pSP/Kv1.3/ cysteine-free (*19*). Engineered cysteines and restriction enzyme sites were introduced into pSP/ΔT1Kv1.3/cysteine-free using the QuikChange Site-Directed Mutagenesis kit. All mutant DNAs were sequenced throughout the entire coding region. Capped cRNA was synthesized in vitro from linearized templates using Sp6 RNA polymerase (Promega, Madison, WI). Linearized templates for Kv1.3 translocation intermediates were generated using several restriction enzymes to produce different length DNA constructs lacking a stop codon (Figure 1B). Proteins were translated in vitro with [^{35}S]methionine (4 μL/50 μL translation mixture; ∼10 μCi/μL Express, Dupont/NEN Research Products, Boston, MA) for 1 h at 22 °C in a rabbit reticulocyte lysate system (2 mM final [DTT]) according to the Promega Protocol and Application Guide.

Pegylation Measurements. As described previously (*19*), translation reaction (40 μL) was added to 500 μL of phosphate-buffered saline (PBS, Ca-free, containing 4 mM $MgCl_2$ (pH 7.3)) with 2 mM DTT. The suspension was centrifuged (Beckman Optima TLX Ultracentrifuge, Beckman TLA 100.3 rotor) through a sucrose cushion (100 μL; 0.5 M sucrose, 100 mM KCl, 5 mM $MgCl_2$, 50 mM Hepes, and 1 mM DTT (pH 7.5)) for 20 min at 70 000 rpm (∼245000*g*) at 4 °C to isolate ribosome-bound peptide. The pellet was resuspended on ice in 90 μL of PBS Ca-free buffer containing 4 mM Mg^{2+} and 100 μM DTT (pH 7.3). A total of 10 μL of buffer containing 10 mM PEG-MAL (5 kDa, Nektar Therapeutics) was added (final PEG-MAL concentration of 1 mM) and incubated at 0 °C for two consecutive time points, 4 and 6 h. Reactions were terminated by addition of 100 mM DTT, followed by incubation of the mixture at room temperature for 10−15 min. Samples were collected

either by centrifugation at 70 000 rpm at 4 °C for 20 min and/or by precipitation with a 90% final volume of cold acid−acetone (900 μL; a stock acid−acetone solution was made by adding 10 μL of HCl to 120 mL of acetone). The final sample was mixed with NuPAGE sample buffer and subjected to SDS−NuPAGE analysis. The fraction of protein pegylated for each residue was calculated as the ratio of counts per minute in the pegylated band (band 1) to the sum of the counts per minute in the pegylated and unpegylated (band 0) bands. If incompletely translated products were present, then the ratio of the full-length to incompletely translated products from the control lane (first lane) was used to correct the amount of pegylation of the full-length nascent peptide. The rate constant for pegylation of K144C was determined as follows. The translation reaction (45 μL) was diluted with 500−800 μL of PBS and centrifuged through a sucrose cushion at 70 000 rpm for 15 min at 4 °C. The pellet was resuspended in PBS buffer containing 0.1 mM DTT and incubated with 1 mM PEG-MAL at 0 °C for 5−240 min, sampling aliquots at appropriate times. Each sample was quenched by addition of 100 mM DTT and subsequent incubation at room temperature for 15 min.

Gel Electrophoresis and Fluorography. All final samples were treated with ∼2 μL of 500 μg/mL RNase for 20 min at room temperature to digest tRNA and remove contaminating peptidyl-tRNA bands. Samples were mixed with NuPAGE sample buffer (1 M glycerol, 0.5 mM EDTA, 73 mM LDS, 141 mM Tris base, and 106 mM Tris-HCl) and heated at 70 °C for 10 min before being loaded onto the gel. Electrophoresis was performed using the NuPAGE system and precast Bis-Tris 10% or 12% gels and MES (50 mM) running buffer (50 mM Tris base, 3.5 mM SDS, and 1 mM EDTA). Gels were soaked in Amplify (Amersham Corp., Arlington Heights, IL) to enhance ^{35}S fluorography, dried, and exposed to Kodak X-AR film at −70 °C. Typical exposure times were 16−30 h. Quantitation of gels was carried out directly using a Molecular Dynamics (Sunnyvale, CA) PhosphorImager.

RESULTS

The structure of Kv1.2 (two subunits only) is shown in Figure 1A, with the T1−S1 linker, the main focus of this investigation, highlighted in red. Below this region is the T1 domain, and above this region is the membrane-integrated region of the channel, including the permeation pore and the voltage-sensing domain. Our strategy for probing the T1−S1 linker was to use native flanking regions with known secondary structures in the mature channel (*4*, *5*, *7*) as controls and to determine structure acquisition intrinsic to the linker itself. We use a mass-tagging cysteine accessibility assay to do this (*19*). The T1 domain acquires tertiary structure as it emerges from the ribosomal exit tunnel and after complete synthesis of the T1−S1 linker has occurred (*17*). A tertiary folded T1 domain outside of the tunnel might sterically hinder access of the modifying reagent to residues in the T1−S1 linker, thereby confounding the interpretation of pegylation. Therefore, to unambiguously measure intrinsic folding of the nascent T1−S1 linker using accessibility assays, we generated a Kv1.3 T1-deleted (ΔT1) mutant (Figure 1B), in which the amino acids of the T1 sequence were deleted and only the C-terminal α-helix of the T1 domain, α5 (blue helix in Figure 1A), remained. Thus, the T1−S1 linker remains nestled between its native N- and C-terminal flanking regions, α5 and S1 (yellow helix in Figure 1A), respectively. These flanking regions serve as controls and validate the use of the ΔT1 mutant (see below). Moreover, there is no evidence that deletion of this domain affects compaction inside the tunnel. This ΔT1 Kv1.3 channel is functionally similar to the full-length wildtype Kv1.3 (*23*, *24*).

The α5 sequence in Kv1.3 is highly identical to that in Kv1.2 (e.g., 92% amino acid identity between Kv1.2 and Kv1.3). Because the α5 sequence exists as an α-helix in the crystal structure of the mature Kv1.2 (*7*), we asked whether the α5 sequence acquires compact secondary structure before it emerges from the ribosomal exit tunnel. To answer this question, we linearized the DNA template at site 179 using an *Nae*I restriction enzyme (Figure 2A). The mRNA transcribed from the DNA template lacks a stop codon; thus, translation of the mRNA produces an arrested nascent peptide that remains attached to the ribosome at site 179 as a translation intermediate. A cysteine scan, one at a time, along the α5 region (residues 142−153) of this nascent peptide was made using standard mutagenesis and then assayed using the PEG-MAL cysteine accessibility methodology (*19*). A peptide that has been mass-tagged with PEG-MAL can be detected on a gel as a 10 kDa or larger shift in mobility (*19*). Because a fully extended peptide occupies 3.0−3.4 Å per amino acid whereas an α-helix occupies 1.5 Å per residue, the length of the peptide when the modifiable cysteine first emerges from the ribosome at the exit site reflects the compactness of the nascent peptide. To completely emerge from the functional ribosomal exit tunnel, a given residue must be 33−34 amino acids, in an extended conformation, from the PTC. The assay is shown in Figure 2B for selected residues between 142 and 153. The first lane in each gel shows a ∼4 kDa peptide. This is the unpegylated parent peptide (labeled "0"). The second and third lanes show the extent of pegylation (labeled "1"), respectively, after 4 and 6 h of treatment with PEG-MAL. The final extent of pegylation was reached within 4 h, as these two lanes gave identical results. The ratio of pegylated (band 1) to the total protein (band 0 + band 1) in each lane is the fraction of nascent peptide labeled. The quantification of pegylation gels is shown in Figure 2C (open circles), along with the results for a molecular tape measure (filled circles) that was previously calibrated and validated as a standard (*19*). This tape measure, which is the C-terminal 44 amino acids of a nascent chain, is all extended and displays monotonically increasing labeling with PEG-MAL as the distance from the PTC increases (*19*). The cysteine-scanned tape measure was positioned to span the length of the ribosomal exit tunnel using the appropriate restriction enzyme and then pegylated. Tape measure residues that are only 26 or 27 amino acids from the PTC are inaccessible to PEG-MAL. Those residues that are ≥33 amino acids from the PTC are >80% labeled with PEG-MAL. Comparison of the labeling curve of an unknown peptide to the tape measure indicates whether the unknown peptide has compact secondary structure. A change in slope and/or a shift of the curve to the right indicates compact secondary structure within the scanned region of the peptide. The region including residues 142−153 appears to be compact, consistent with crystal structures of the T1 domain (*4*, *5*, *7*). Residue 153C is inaccessible to PEG-MAL, whereas 142C, which is 38 amino acids away from the PTC,

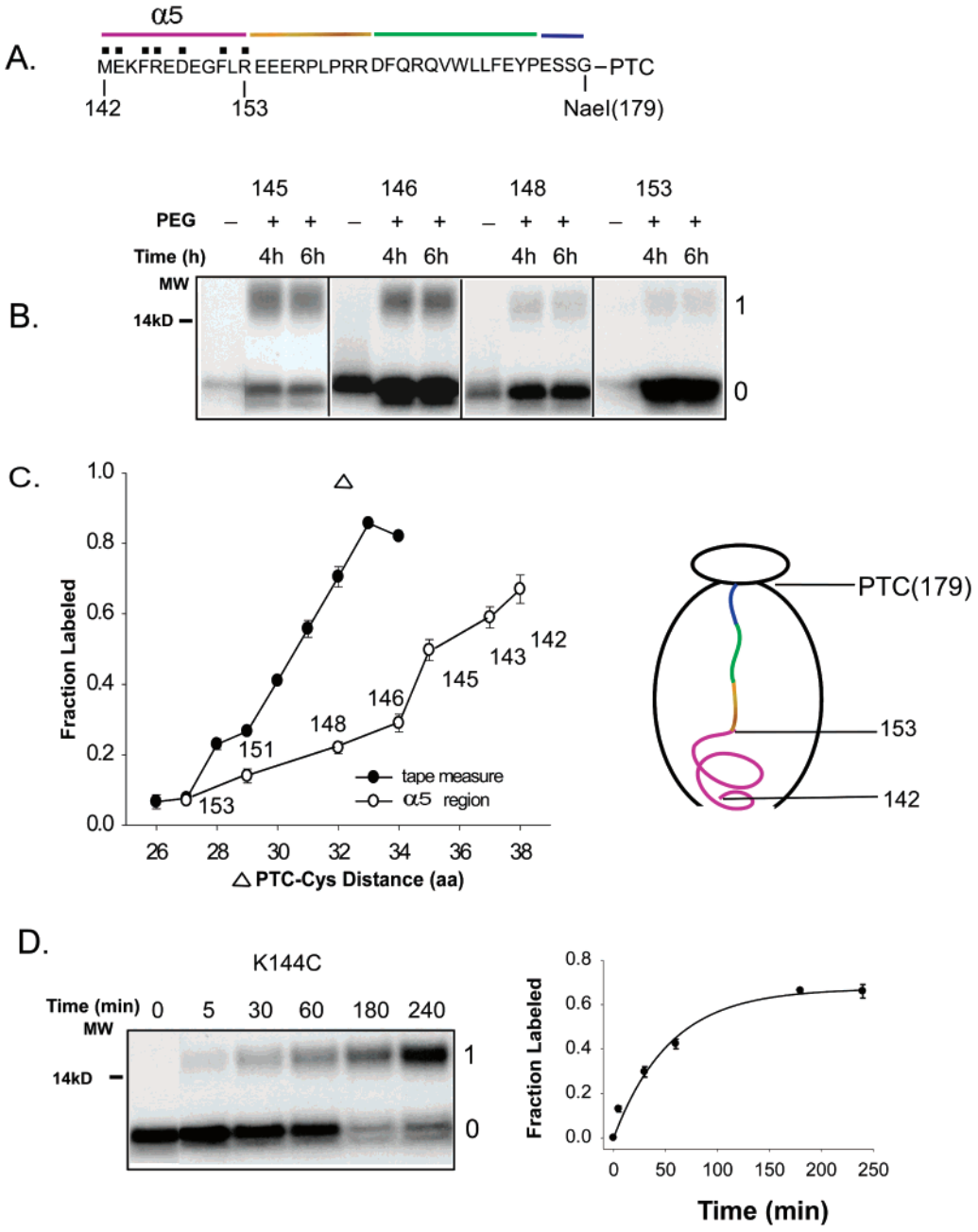

FIGURE 2: Accessibility of the N-terminal region of the T1−S1 linker (α5). (A) Schematic drawing of the *Nae*I (179)-cut construct. The amino acid sequence is indicated by a single-letter code. Cysteine substitution residues are marked by a square dot. The number under the letter code corresponds to the amino acid in the native full-length sequence of Kv1.3, and colored bars represent the different segments of the α5 and T1−S1 linker. (B) Extent of pegylation of α5 residues. The first lane for each indicated cysteine residue shows samples that contained no PEG-MAL and was used as the zero time point. The second and third lanes for each residue show samples incubated with 1 mM shows samples that PEG-MAL for 4 and 6 h, respectively, at 0 °C. Gels were 12% NuPAGE Bis-Tris with MES running buffer. Numbers to the left of the gel are MW standards; numbers to the right of the gel indicate unpegylated (0) and singly pegylated (1) protein. (C) Fraction of Kv1.3 nascent peptide labeled. The *x*-axis is the number of amino acids from the PTC site to (and including) the labeled cysteine. Pegylation of a known extended peptide; the tape measure is shown by the filled circle and represents data taken from ref *19*. The final extent of pegylation of α5 residues is represented by the open circles. Data are shown as mean ± SEM (n = 3−5). To test for any decrease in reactivity of a cysteine in the tunnel, we determined the fraction labeled with PEG-MAL following treatment with a small maleimide that can diffuse into the tunnel (open triangle). Nascent peptide was treated with 0.5 mM phenyl dimaleimide for 20 min at 0 °C, quenched with 10 mM β-mercaptoethanol at room temperature for 15 min, and centrifuged. The pellet was resuspended in PBS buffer containing 1 mM β-mercaptoethanol, 10 μg/mL RNase and incubated for 20 min at room temperature and then pegylated as described in Materials and Methods. The fraction pegylated indicates that the reactivity of the cysteine in the tunnel is unimpaired. The cartoon indicates an interpretation of the data: residues 142−153 form a compact structure (α-helix) near the bottom part of exit tunnel (dark red helical line). (D) Pegylation time course of K144C. Translation products were diluted into pegylation buffer, incubated with 1 mM PEG-MAL for the indicated time, quenched with 50 mM DTT, and assayed on a gel. The left panel shows the unmodified and singly modified peptide at each time. A 12% Bis-Tris gel with MES running buffer was used in the NuPAGE system. Unpegylated protein is labeled as "0" and singly pegylated protein is labeled as "1". The right panel shows the fraction modified plotted as a function of time of PEG-MAL exposure. The data were fit with single-exponential function to give a rate constant of ∼0.31 ± 0.06 M^{-1} s^{-1} for K144C (mean ± SEM, n = 3).

was ∼70% pegylated. Residue 148C, which is 32 residues away from the PTC, was only ∼20% pegylated. In contrast, a tape measure residue that is 32 amino acid from the PTC is ∼70% pegylated. This decreased pegylation is due to a decreased accessibility of 148C to PEG-MAL, rather than a decreased reactivity, because a small maleimide, phenyl dimaleimide, completely labels this residue in the nascent peptide (open triangle, Figure 2C). There is a monotonic increase in the apparent accessibility between positions 153 and 142. In contrast, the region including residues 153−179 is extended because these 26 residues coincide with the tape measure and do not contribute to a shift in the base of the length-dependent pegylation curve.

What does change relative to the tape measure, however, is the slope of this curve between residue 153 and 142. This decrease in extent of labeling with distance from PTC suggests that the α5 region acquires a compact structure inside the ribosomal exit tunnel, near the exit port. The data for the tape measure and α5 cross at approximately a ΔPTC-cysteine distance of 27 residues. It takes five residues from this point for the tape measure to reach ∼70% pegylation, a distance of ∼15−17 Å, but 11 residues for α5 to traverse the same distance. This distance, divided by 11 amino acids, yields ∼1.5 Å per amino acid, which describes an α-helix. Thus, it is likely that the α5 region from 153 to 142 is an α-helix. The propensity of residues 142−153 to form a compact structure may be enhanced by the presence of charged side-chains, e.g., positively charged residues K144, R153 and negatively charged residues E147, D148, and E149, which could potentially form at least two salt-bridges. Charge pair interactions are known to stabilize α-helical conformations of alanine-based peptides in solution, especially when the charged residues are separated by two or three intervening amino acids (*25*). Thus, a salt-bridge or ion pair might help to stabilize the compact conformation detected in the 142−153 region. If a charge-altering mutation of K144 disrupts this interaction and destabilizes the α-helical structure, then a more extended conformation will be present. Consistent with this hypothesis, K144C is ∼70% pegylated (Figure 2D), similar to the more distally located 142C. On the basis of a calibration of 3−3.4 Å per amino acid for the extended tape measure (*19*), 70% pegylation of K144C suggests that it is located ∼96−109 Å from the PTC. The pegylation time course (Figure 2D) further supports this conclusion: the pegylation rate constant of K144C is 0.31 M^{-1} s^{-1}, similar to the value obtained for a tape measure residue at this same distance from the PTC (*19*). These results suggest that charge pair formation may lower the free energy of α5 helix formation. A positively charged side-chain at this position is conserved in most Kv1 family members, as is the presence of negatively charged residues separated from a positive charge by two or three intervening amino acids. This will be the subject of future investigation.

The S1 Transmembrane Segment. Having shown that the N-terminal flanking region of the T1−S1 linker (α5 region) forms a compact structure in the nascent chain inside the tunnel, we asked whether the C-terminal flanking region, S1, could also compact inside the tunnel. S1 is an α-helix in the mature Kv channel (*26*−*28*), but it is not known when, and in which compartment, this helicity is first manifested. Two general locations in the tunnel, proximal to the exit port and proximal to the PTC, were investigated. First, we positioned the S1 segment near the exit port by linearizing the DNA template with a *Bst*BI restriction enzyme (Figure 3A), and then cysteine-scanned S1 from 180 to195. The pegylation reaction products are shown in Figure 3B for selected residues. Residue 183C is almost completely pegylated, whereas residue 195C is mostly unpegylated. Quantification of the data and comparison of the length-dependent pegylation for S1 and the tape measure shows that the N-terminal half of S1 (residues 183−193) is much less sensitive, i.e., the slope of the length-dependent pegylation curve is decreased relative to that of the tape measure (Figure 3C). This suggests that the N-terminal half of the S1 (183−193) acquires a compact secondary structure inside the tunnel. Residue 189C is 34 residues away from the PTC and yet is only ∼50% pegylated. The corresponding tape measure residue that is 34 amino acids away from the PTC is ∼80% pegylated. It takes almost twice as many residues for S1 (vs the tape measure) to span a similar distance inside the tunnel, suggesting that this segment of S1 is helical in this location of the tunnel. The decreased pegylation for residues 183−193 compared with the tape measure is not due to block of the ribosomal exit tunnel by the N-terminal nascent peptide, i.e., α5 and the T1−S1 linker. Such a scenario would produce a significant right shift of the bottom part of the length-dependence curve for labeling. This is not observed. Quite the contrary, the C-terminal half of S1, residues 193C and 195C, which are located even deeper into the tunnel, exactly coincides with the tape measure. Thus, the C-terminal segment of S1 does not form a compact structure in this location of the tunnel, nor does the N-terminal half of the S1−S2 loop (residues 202−222). The nascent chain from 193 to 222 is extended.

The location of the peptide in the tunnel influences secondary folding (*20*). Thus, although S1 compacts near the exit port of the tunnel, this does not mean that it compacts all along the tunnel. For example, does the N-terminal half of S1 compact near the PTC, the position it occupies when first synthesized? This region of the tunnel is permissive for helix formation (*15*, *20*, *21*). To determine whether the N-terminal half of S1 acquires a compact structure near the PTC, we engineered a nascent peptide arrested at site 194, which positions residues 183−193 adjacent to the PTC (Figure 4A). In this nascent peptide, 162C is 33 amino acids away from the PTC and serves as a reporter residue. If the N-terminal half of S1 (183−193) does compact, then this will cause retraction of the reporter residue 162C into the ribosomal tunnel, making 162C less accessible, resulting in less pegylation (*19*). If there is no compaction of S1 near the PTC, then the amount of pegylation of 162C will be similar to that of the tape measure. Figure 4B shows that 162C, as well as 144C (51 residues from the PTC), are 80% pegylated. Both residues reach the maximum pegylation compared to the tape measure. These results indicate that the residues from 183 to 193, located adjacent to the PTC, do not acquire a compact structure, nor do residues 162−182. Both regions are extended in this location in the tunnel. Therefore, further scanning was not done on this construct.

The T1−S1 linker. Both flanking regions of the T1−S1 linker form compact structures near the bottom part of ribosomal exit tunnel, before they completely leave the tunnel. Does the intervening T1−S1 linker itself compact in the tunnel? The results shown in Figure 4B already provide

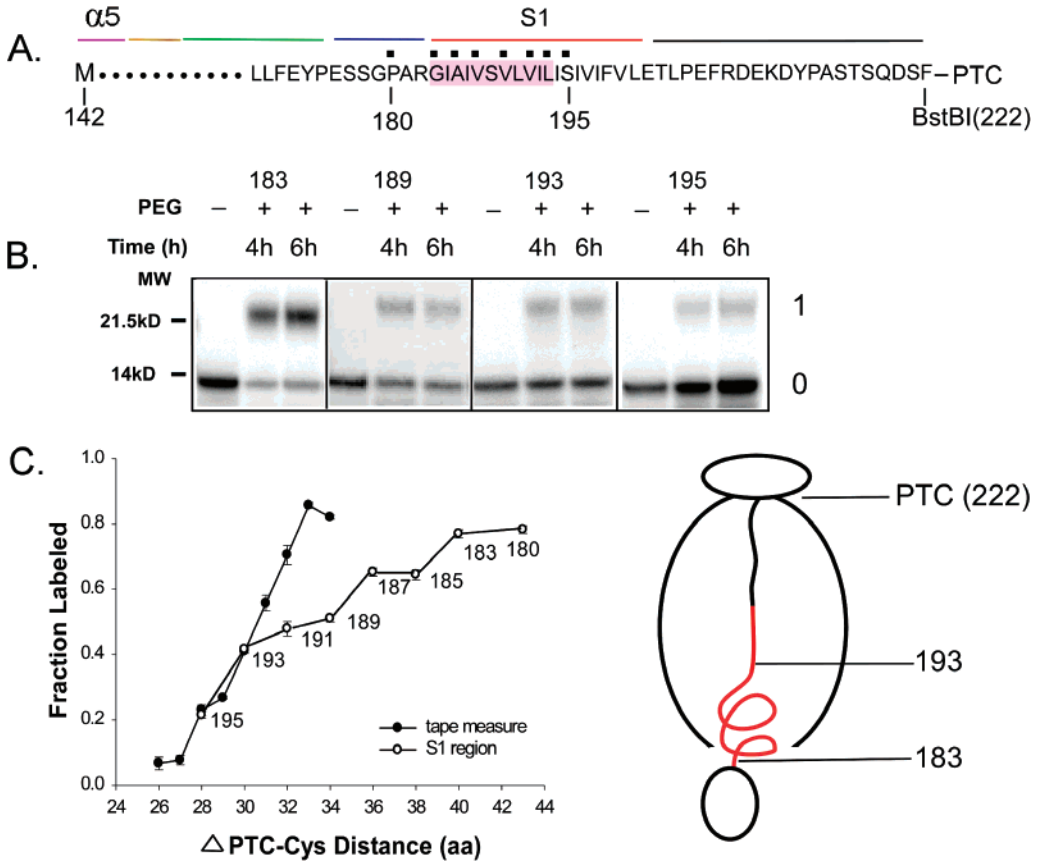

FIGURE 3: Accessibility of S1 located distal to the PTC. (A) Schematic drawing of the *Bst*EII (222)-cut construct. The amino acid sequence is indicated by a single-letter code. Long stretches of amino acids present in the construct but omitted from the diagrammed sequence are indicated by ellipses (....). Cysteine substitution residues are marked by a square dot. The number under the letter code corresponds to the amino acid in the native full-length sequence in Kv1.3, and colored bars represent the different segments of the α5 helix, T1−S1 linker, and S1 segment. (B) Extent of pegylation of S1 residues. Samples and conditions are as described in Figure 2B. Three lanes depict unpegylated (0) and singly pegylated (1) nascent peptide at three time points: 0, 4, and 6 h, for each cysteine. (C) Fraction of Kv1.3 nascent peptide labeled. The data shown in B are plotted, as described in Figure 2C, for each cysteine indicated, along with the length-dependent pegylation for the tape measure. The cartoon indicates an interpretation of the data: the N-terminus of S1, residues 183−193, forms an α-helix. The circle indicates a peptide segment whose structure is unknown outside the ribosomal tunnel.

an answer regarding the secondary structure of the linker near the bottom of the tunnel. Residue 162 is 33 residues from the PTC and is 80% pegylated, indicating that the entire chain from 162 to 194 is extended. This includes all but the first eight residues (153−161) of the T1−S1 linker plus the N-terminal segment of S1. To complete our analysis of the T1−S1 linker, we engineered residues 153−162 to reside in the bottom part of the exit tunnel by linearizing the DNA template with a *Nru*I restriction enzyme (Figure 5A), which attaches the nascent chain to the PTC at position 188. A cysteine scan of residues 151−162 shows that 156C, which is 33 residues form the PTC, is almost entirely pegylated, whereas 162C is almost entirely unpegylated (Figure 5B). A plot of the fraction labeled versus distance from the PTC superimposes on the curve of the all-extended tape measure (Figure 5C), indicating that the region containing residues 156−188 is extended.

Finally, to address whether the T1−S1 linker would compact if repositioned even further near the exit port, residues 168−175 were engineered to reside at the bottom of the tunnel by linearizing with an *Xba*I restriction enzyme, which attaches the nascent chain at position 201 (Figure 6A). Residue 175C is relatively inaccessible to PEG-MAL (<20% pegylated), whereas 169C is maximally accessible (>80% pegylated; Figure 6B). As shown in Figure 6C, the curve for the entire cysteine-scanned region superimposes on the tape measure curve, consistent with an all-extended region between 168 and 201.

The T1−S1 linker is extended when located in four different regions of the tunnel and in nascent peptides of various chain lengths. Taken together, these results suggest that the entire T1−S1 linker does not form a compact secondary structure before it emerges from the functional ribosomal exit tunnel.

DISCUSSION

Although the crystal structure of the whole tetrameric Kv1.2 channel (*7*) has provided invaluable insights into the structure and function of Kv channels, several issues remain unresolved. For example, the resolution of the T1−S1 linker and that of S1 structure are quite low, and assignments and registers cannot be made. Regardless, there is no doubt that the S1 transmembrane segment of mammalian Kv channels has an α-helical structure in the mature functional channel. This is confirmed from noncrystallographic evidence for mammalian Kv channels (*26*, *27*) and consistent with crystallographic results for a prokaryotic Kv channel (*28*). In contrast, the secondary structure of the T1−S1 linker is equivocal but has been suggested to be helical (*7*). Our results indicate that the T1−S1 linker lacks its own intrinsic signal

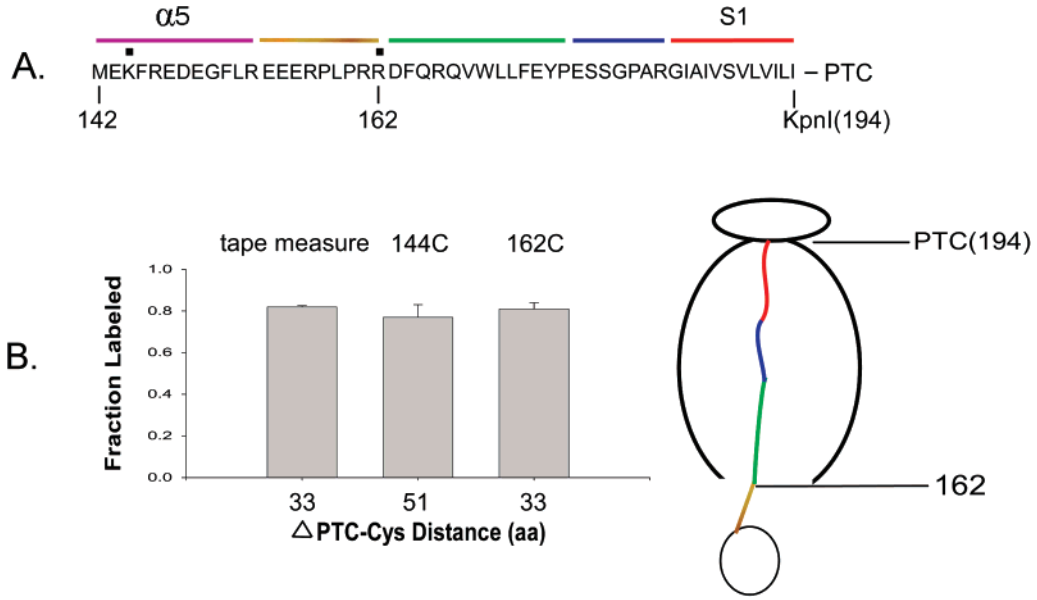

FIGURE 4: N-terminus of S1 located proximal to the PTC. (A) Schematic drawing of the *Kpn*I (194)-cut construct. The amino acid sequence is indicated by a single-letter code. Cysteine substitution residues are marked by a square dot. The number under the letter code corresponds to the amino acid in the native full-length sequence in Kv1.3 and colored bars represent the different segments of the α5, T1−S1 linker, and S1 segment. (B) Fraction of Kv1.3 nascent peptide labeled. Data are means ± SEM ($n = 3$). The final fraction of labeling of 144C and 162C were each ~0.8, not significantly different from the tape measure control. The cartoon indicates an interpretation of the data: residues 162−194 do not form a compact structure. The circle indicates a peptide segment whose structure is unknown outside the ribosomal tunnel.

for helix formation, suggesting that if the helical structure proposed by Long et al. for Kv1.2 (*7*) does indeed exist in the mature channel, then both tertiary and quaternary interactions facilitate helix formation of the T1−S1 linker.

The T1 Domain. Here, we report that the C-terminal portion of the T1 domain (residues from 142 to 153) does form a compact structure inside the bottom portion of the functional ribosomal exit tunnel. This region of the T1 domain corresponds to the α5 helix observed in mature Kv channels (*7*) and in the isolated T1 domain (*4*). In our experiments, this C-terminal portion of the T1 domain serves as a positive control (calibration) for helix formation near the exit port of the ribosomal tunnel. We conclude that residues 142−153 form an α-helix because the length-dependent extent of pegylation is significantly right-shifted with respect to the tape measure. The slope of this curve is not abrupt, but gradual, which is to be expected and has been discussed previously (*19*). Almost twice as many amino acids are required to span the last 20 Å of the tunnel as are required for the tape measure (*19*), consistent with the formation of an α-helical structure. These results agree with our earlier estimates of structure formation of the nascent T1 domain (*17*). Moreover, these results suggest that the α5 helix can form independently of the α4 helix, with which it forms a helical hairpin in the mature T1 domain (*4*, *7*, *29*), because α4 is not present in the ΔT1 nascent peptide used in these studies. In addition, intrahelix charge pair interaction may play a role in stabilizing T1 helices in Kv1.3. Because most of the α-helices in T1 have the appropriate intrahelical charge distribution for charge-pair interaction, this conclusion may apply to T1 helices other than α5.

The S1 Transmembrane Segment. The S1 transmembrane segment, which is highly conserved in Kv channels, has a α-helical structure, as determined by tryptophan- and alanine-scanning studies (*26*, *27*) and as depicted in the crystal structure of Kv 1.2 (*7*). The S1 segment alone integrates extremely efficiently, with correct orientation, into the lipid bilayer (*30*), suggesting that secondary structure acquisition occurs prior to, or during, insertion of this segment into the ER membrane. Moreover, transmembrane Kv segments cooperate during Kv topogenesis and assembly to modulate integration and translocation efficiencies of the transmembrane segments (*30*). These cooperative interactions might occur at the level of the translocon and the bilayer, or perhaps even at the level of the ribosome, and involve the ability of transmembrane segments to acquire compact secondary structure. For Kv channels to pass quality control and exit the ER, the channel must achieve correct secondary, tertiary, and quaternary folding. This raises the issue of when and in which compartment the first transmembrane segment, S1, of a polytopic protein acquires its proper structure. Does it form a helix while in the ribosomal tunnel or at some subsequent stage that perhaps requires tertiary or quaternary interactions with the rest of the Kv channel, the translocon, or the lipid bilayer? Our studies bear on this question and specifically test whether S1 forms a compact structure inside the ribosomal tunnel.

Precedent exists for helix formation in the tunnel (*14*, *15*−*20*). More specifically, precedent exists for helix formation of a transmembrane segment of Kv1.3 in the tunnel. We previously found that the S6 transmembrane segment of Kv1.3 forms an α-helical structure inside the ribosomal tunnel (*19*). Our present results suggest that S1 starts to compact before it completely emerges from the ribosomal tunnel. For residues from 183 to 193, the N-terminal half of S1, the length-dependent extent of pegylation is right-shifted from that of the tape measure and requires almost twice the number of residues as the tape measure to span the last 20 Å of the tunnel. Thus, the region between 183 and 193 is compact and likely helical. Interestingly, this region only forms a compact structure inside the ribosomal tunnel near the exit port, but not in the tunnel near the PTC. When S1

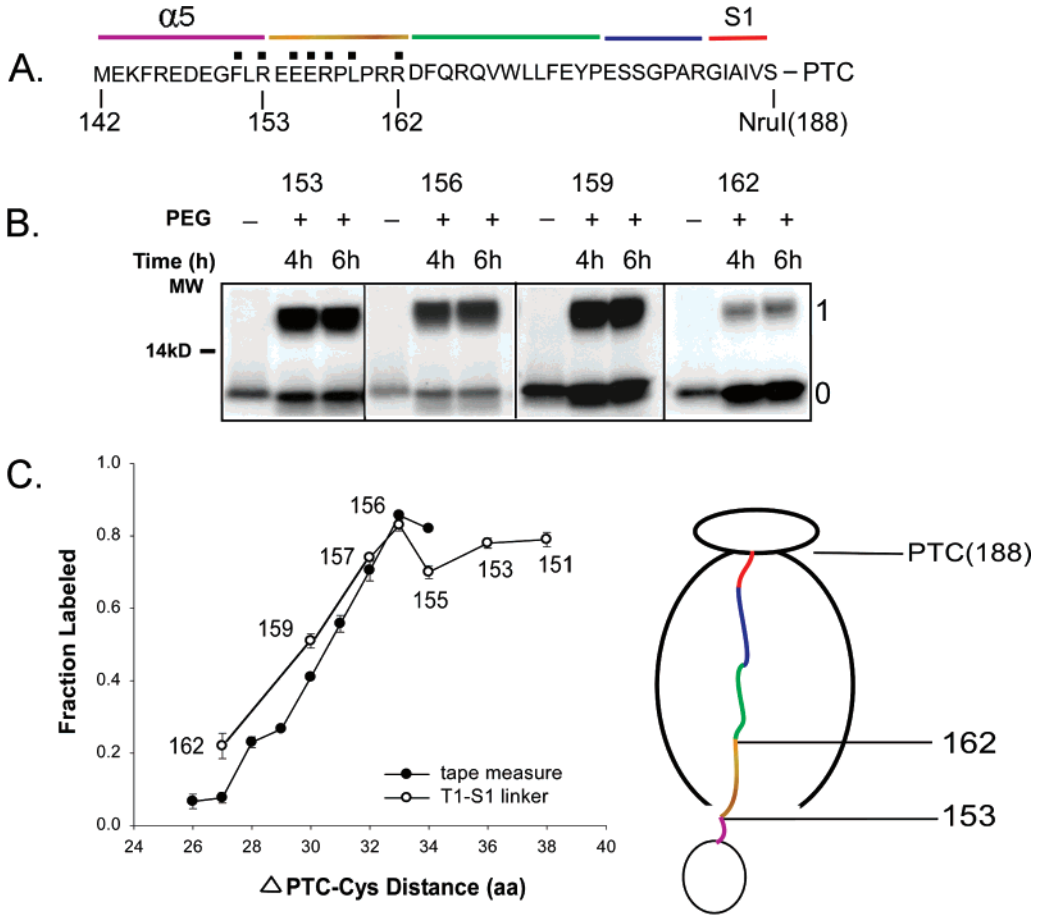

FIGURE 5: Accessibility of N-terminal region in the T1−S1 linker. (A) Schematic drawing of the *Nru*I (188)-cut construct. The amino acid sequence is indicated by a single-letter code. Cysteine substitution residues are marked by a square dot. The number under the letter code corresponds to the amino acid in the native full-length sequence in Kv1.3, and colored bars represent the different segments of the α5, T1−S1 linker, and S1 segment. (B) Extent of pegylation of T1−S1 linker residues. Samples and conditions are as described in Figure 2B. Three lanes depict unpegylated (0) and singly pegylated (1) nascent peptide at three time points: 0, 4, and 6 h, for each cysteine. (C) Fraction of Kv1.3 nascent peptide labeled. The data shown in B are plotted, as described in Figure 2C, for each cysteine indicated, along with the tape measure control. The cartoon indicates an interpretation of the data: residues 156−188 are extended. The circle indicates a peptide segment whose structure is unknown outside the ribosomal tunnel.

is located within 60 Å of the PTC (Figures 4 and 6), it is extended. This lack of compaction is not due to the absence of the C-terminal half of S1 because the *Xba*I-cut construct (Figure 6) contains the C-terminal half of S1, yet this peptide is extended. When it is located more than 80 Å away from the PTC, it is compact and likely helical. In both cases, the C-terminal half of S1 is present. Compaction appears to depend on both the nature of the peptide sequence and the region of the tunnel because other peptide sequences can compact near the PTC (*15*, *19*, *20*). The C-terminal segment of S1, residues 194−201, is extended because the length-dependence of pegylation is similar to that of the tape measure. In S6, the C-terminal half, in contrast to the N-terminal half, also shows no compaction in this same location of the tunnel. Taken together, these results suggest that (i) the S1 segment of Kv1.3 can form an α-helical structure before it fully emerges from the ribosomal tunnel, (ii) both S1 and S6 (*19*) compact in the bottom part of the ribosomal tunnel, and (iii) different transmembrane sequences may have their own preferred tunnel region in which to form compact structures.

The T1−S1 Linker. The T1−S1 linker connects the T1 recognition domain to the first transmembrane segment of the channel. As mentioned above, MacKinnon and co-workers could not assign the residues in this region of the electron density map of their X-ray crystallographic study of Kv1.2, nor is the register of this linker, or of S1, known (*7*). The disordered T1−S1 region reported for the Kv1.2 crystal structure may reflect a region with intrinsic disorder, a region that assumes different positions as a rigid structure, or may be a consequence of technical difficulties (*31*). Because the T1−S1 linker in Kv1.2 contains ∼33 amino acids, MacKinnon and co-workers modeled the linker as two polyglycine α-helices (*7*), thereby compressing the 33 residues into the space between T1 and S1. This distance can also be spanned by ≥16 linker residues in an all-extended conformation (3.0−3.4 Å/residue for an extended peptide) with or without tertiary structure. Alternatively, the T1−S1 linker could include a combination of helical and extended conformations. Regardless, whether or not the linker is helical in the mature Kv structure, we can ask whether the T1−S1 linker forms a compact structure in the nascent Kv monomer. Our results show that the T1−S1 linker does not compact inside the ribosomal tunnel, regardless of where it is located along the tunnel. In contrast, regions flanking the T1−S1 linker, α5 and S1, each acquire compact structures before completely emerging from the tunnel.

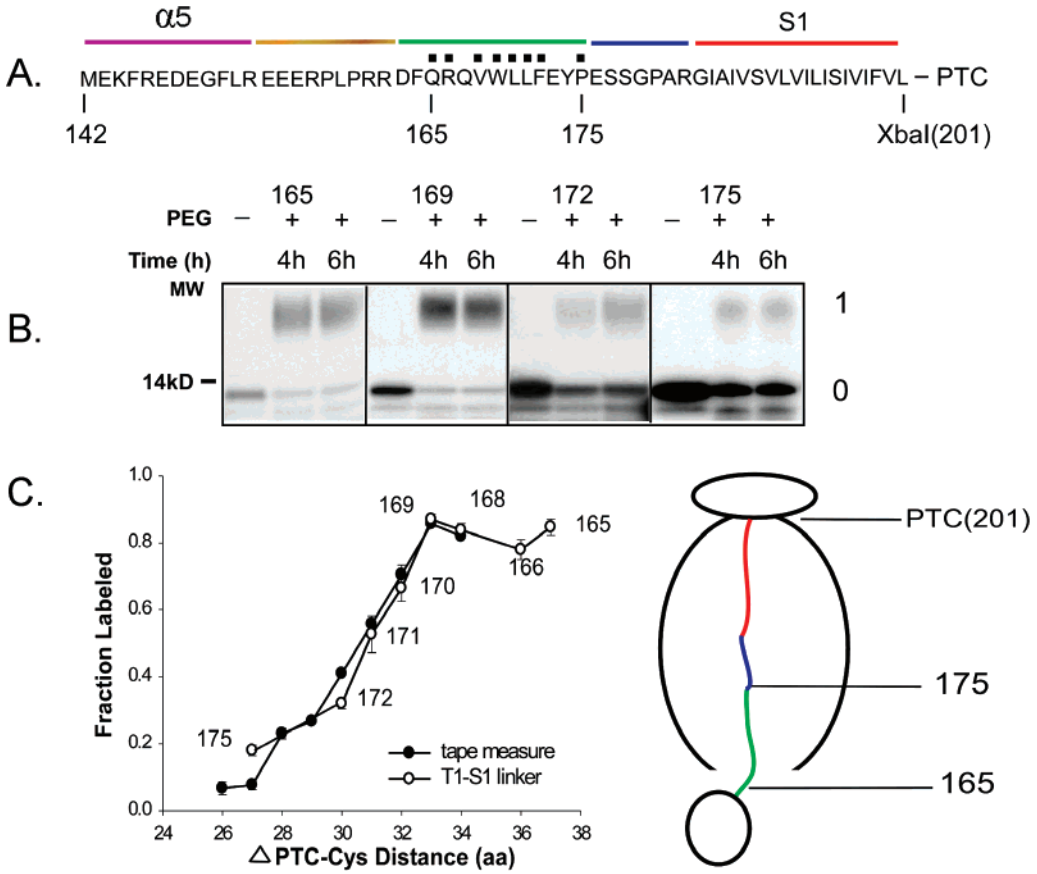

FIGURE 6: Accessibility of T1−S1 linker residues from 165 to 175. (A) Schematic drawing of the *Xba*I (201)-cut construct. The amino acid sequence is indicated by a single-letter code. Cysteine substitution residues are marked by a square dot. The number under the letter code corresponds to the amino acid in the native full-length sequence in Kv1.3, and colored bars represent the different segments of the α5, T1−S1 linker, and S1 segment. (B) Extent of pegylation of T1−S1 linker residues. Samples and conditions are as described in Figure 2B. Three lanes depict unpegylated (0) and singly pegylated (1) nascent peptide at three time points: 0, 4, and 6 h, for each cysteine. (C) Fraction of Kv1.3 protein labeled. The data shown in B are plotted, as described in Figure 2C, for each cysteine indicated, along with the tape measure control. The cartoon indicates an interpretation of the data: residues 168−201 are extended. The circle indicates a peptide segment whose structure is unknown outside the ribosomal tunnel.

Why does the T1−S1 linker not form an α-helix inside the tunnel? There are two basic reasons. First, it is possible that the T1−S1 linker is not helical in the mature channel. Second, it is possible that helix formation occurs at a later stage of biogenesis, perhaps coupled to tertiary and/or quaternary structure formation of the channel. Using AGADIR, a helix propensity algorithm that predicts the helicity for soluble proteins (*32*), we can infer the helix propensity of the T1−S1 linker sequence. Regions 154−162 and 173−182 do not have any helix propensity, whereas the region including 163−172 has a helix propensity similar to that calculated for the α5 sequence. If the T1−S1 linker does form a helix in the final mature protein, then deferred folding could be tied to explicit functions of the T1 domain. For example, T1 serves as a recognition and tetramerization domain (*23*, *33*−*37*), and the length of the T1−S1 linker plays an important role in the channel's functional expression (*38*). Although deletion of the T1 domain from several Kv isoforms still permits functional channels to be expressed, the efficiency is quite low (*24*, *33*, *39*−*42*). Moreover, deletion of the T1−S1 linker in Kv1.1a prevents the appearance of functional channels (*38*). Even partial deletion of different regions of the T1−S1 linker abolishes functional channel formation. These deletion mutants cannot be rescued by coexpression with full-length channel subunits (*38*). Similar results were found for Kv1.3 (Tu and Deutsch, unpublished data). These studies suggest that the T1−S1 linker is important for channel expression, perhaps by facilitating T1 domain tetramerization. In Kv1.3, tetramerization proceeds via a T1−T1 dimerization pathway (*43*), and this T1−T1 interaction occurs early in Kv biogenesis, likely in the ER while nascent peptides are still attached to the ribosome (*44*). We therefore propose that a relatively long and flexible T1−S1 linker may favor a T1−T1 interaction necessary for oligomerization, since an extended structure at this stage of biogenesis would yield a more flexible T1−S1 linker chain with approximately twice the length of the corresponding α-helix. The advantage of having a long, flexible linker at early stages of biogenesis may be that it permits speedy exploration of configurations for finding T1−T1 interactions, a so-called "fly casting" mechanism (*45*). At later stages of biogenesis, formation of the final structure of the T1−S1 linker may be coupled to tetramerization of T1, the pore, and/or voltage-sensor domains, as well as more extensive tertiary and quaternary folding (*30*, *46*).

ACKNOWLEDGMENT

We thank Drs. Richard Horn, LiQiong Chen, and Wei Wang, for critical reading of the manuscript.

REFERENCES

1. Hille, B. (2001) *Ion Channels of Excitable Membranes*; Sinauer Associates, Inc.: Sunderland, MA.
2. Ashcroft, F. M. (2000) *Ion Channels and Disease*; Academic Press, San Diego.
3. Kreusch, A., Pfaffinger, P. J., Stevens, C. F., and Choe, S. Crystal structure of the tetramerization domain of the *Shaker* potassium channel, *Nature* 392, 945−948.
4. Minor, D. L., Lin, Y. F., Mobley, B. C., Avelar, A., Jan, Y. N., Jan, L. Y., and Berger, J. M. (2000) The polar T1 interface is linked to conformational changes that open the voltage-gated potassium channel, *Cell 102*, 657−670.
5. Gulbis, J. M., Zhou, M., Mann, S., and MacKinnon, R. (2000) Structure of the cytoplasmic beta subunit-T1 assembly of voltage-dependent K^+ channels, *Science 289*, 123−127.
6. Kobertz, W. R., Williams, C., and Miller, C. (2000) Hanging gondola structure of the T1 domain in a voltage-gated K^+ channel, *Biochemistry 39*, 10347−10352.
7. Long, S. B., Campbell, E. B., and MacKinnon, R. (2005) Crystal structure of a mammalian voltage-dependent *Shaker* family K^+ channel, *Science 309*, 897−903.
8. Sokolova, O., Kolmakova-Partensky, L., and Grigorieff, N. (2001) Three-dimensional structure of a voltage-gated potassium channel at 2.5 nm resolution, *Structure 9*, 215−220.
9. Ban, N., Nissen, P., Hansen, J., Moore, P. B., and Steitz, T. A. (2000) The complete atomic structure of the large ribosomal subunit at 2.4 Å resolution, *Science 289*, 905−920.
10. Nissen, P., Hansen, J., Ban, N., Moore, P. B., and Steitz, T. A. (2000) The structural basis of ribosome activity in peptide bond synthesis, *Science 289*, 920−930.
11. Beckmann, R., Spahn, C. M., Eswar, N., Helmers, J., Penczek, P. A., Sali, A., Frank, J., and Blobel, G. (2001) Architecture of the protein-conducting channel associated with the translating 80S ribosome, *Cell 107*, 361−372.
12. Menetret, J. F., Neuhof, A., Morgan, D. G., Plath, K., Radermacher, M., Rapoport, T. A., and Akey, C. W. (2000) The structure of ribosome-channel complexes engaged in protein translocation, *Mol. Cell 6*, 1219−1232.
13. Voss, N. R., Gerstein, M., Steitz, T. A., and Moore, P. B. (2006) The geometry of the ribosomal polypeptide exit tunnel, *J. Mol. Biol. 360*, 893−906.
14. Mingarro, I., Nilsson, I., Whitley, P., and von Heijne, G. (2000) Different conformations of nascent polypeptides during translocation across the ER membrane, *BMC Cell Biol. 1*, 3.
15. Woolhead, C. A., McCormick, P. J., and Johnson, A. E. (2004) Nascent membrane and secretory proteins differ in FRET-detected folding far inside the ribosome and in their exposure to ribosomal proteins, *Cell 116*, 725−736.
16. Kowarik, M., Kung, S., Martoglio, B., and Helenius, A. (2002) Protein folding during cotranslational translocation in the endoplasmic reticulum, *Mol. Cell 10*, 769−778.
17. Kosolapov, A., Tu, L., Wang, J., and Deutsch, C. (2004) Structure acquisition of the T1 domain of Kv1.3 during biogenesis, *Neuron 44*, 295−307.
18. Hardesty, B., and Kramer, G. (2001) Folding of a nascent peptide on the ribosome, *Prog. Nucleic Acid Res. Mol. Biol. 66*, 41−66.
19. Lu, J., and Deutsch, C. (2005) Secondary structure formation of a transmembrane segment in Kv channels, *Biochemistry 44*, 8230−8243.
20. Lu, J., and Deutsch, C. (2005) Folding zones inside the ribosomal exit tunnel, *Nat. Struct. Mol. Biol. 12*, 1123−1129.
21. Woolhead, C. A., Johnson, A. E., and Bernstein, H. D. (2006) Translation arrest requires two-way communication between a nascent polypeptide and the ribosome, *Mol. Cell 22*, 587−598.
22. Lu, J., and Deutsch, C. (2001) Pegylation: a method for assessing topological accessibilities in Kv1.3, *Biochemistry 40*, 13288−13301.
23. Tu., L., Santarelli, V., and Deutsch, C. (1995) Truncated K^+ channel DNA sequences specifically suppress lymphocyte K^+ channel gene expression, *Biophys. J. 68*, 147−156.
24. Tu, L., Santarelli, V., Sheng, Z.-F., Skach, W., Pain, D., and Deutsch, C. (1996) Voltage-gated K^+ channels contain multiple intersubunit association sites, *J. Biol. Chem. 271*, 18904−18911.
25. Marqusee, S., and Baldwin, R. L. (1987) Helix stabilization by Glu^-...Lys^+ salt bridges in short peptides of de novo design, *Proc. Natl. Acad. Sci. U.S.A. 84*, 8898−8902.
26. Hong, K. H., and Miller, C. (2000) The lipid-protein interface of a *Shaker* K^+ channel, *J. Gen Physiol. 115*, 51−58.
27. Li-Smerin, Y., Hackos, D. H., and Swartz, K. J. (2000) Alpha-helical structural elements within the voltage-sensing domains of a K^+channel, *J. Gen. Physiol. 115*, 33−50.
28. Jiang, Y., Lee, A., Chen, J., Ruta, V., Cadene, M., Chait, B. T., and MacKinnon, R. (2003) X-ray structure of a voltage-dependent K^+ channel, *Nature 423*, 33−41.
29. Kosolapov, A., and Deutsch, C. (2006) Folding of T1 subdomains of nascent Kv1.3, *FASEB J. 20*, A965.
30. Tu, L., Wang, J., Helm, A., Skach, W. R., and Deutsch, C. (2000) Transmembrane biogenesis of Kv1.3, *Biochemistry 39*, 824−836.
31. Dunker, A. K., Lawson, J. D., Brown, C. J., Williams, R. M., Romero, P., Oh, J. S., Oldfield, C. J., Campen, A. M., Ratliff, C. M., Hipps, K. W., Ausio, J., Nissen, M. S., Reeves, R., Kang, C., Kissinger, C. R., Bailey, R. W., Griswold, M. D., Chiu, W., Garner, E. C., and Obradovic, Z. (2001) Intrinsically disordered protein, *J. Mol. Graph. Model. 19*, 26−59.
32. Munoz, V., and Serrano, L. (1997) Development of the multiple sequence approximation within the AGADIR model of alpha-helix formation: comparison with Zimm-Bragg and Lifson-Roig formalisms, *Biopolymers 41*, 495−509.
33. Shen, N. V., Chen, X., Boyer, M. M., and Pfaffinger, P. (1993) Deletion analysis of K^+ channel assembly, *Neuron 11*, 67−76.
34. Lee, T. E., Phillipson, L. H., Kuznetsov, A., and Nelson, D. J. (1994) Structural determinant for assembly of mammalian K^+ channels, *Biophys. J. 66*, 667−673.
35. Babila, T., Moscucci, A., Wang, H., Weaver, F. E., and Koren, G. (1994) Assembly of mammalian voltage-gated potassium channels: Evidence for an important role of the first transmembrane segment, *Neuron 12*, 615−626.
36. Xu, J., Yu, W., Jan, J. N., Jan, L., and Li, M. (1995) Assembly of voltage-gated potassium channels. Conserved hydrophilic motifs determine subfamily-specific interactions between the α-subunits, *J. Biol. Chem. 270*, 24761−24768.
37. Shen, N. V., and Pfaffinger, P. J. (1995) Molecular recognition and assembly sequences involved in the subfamily-specific assembly of voltage-gated K^+ channel subunit proteins, *Neuron 14*, 625−633.
38. Hopkins, W. F., Demas, V., and Tempel, B. L. (1994) Both N- and C-terminal regions contribute to the assembly and functional expression of homo- and heteromultimeric voltage-gated K^+ channels, *J. Neurosci. 14*, 1385−1393.
39. Van Dongen, A. M. J., Frech, G. C., Drewe, J. A., Joho, R. H., and Brown, A. M. (1990) Alteration and deletion of K^+ channel function by deletions at the N- and C-temini, *Neuron 5*, 433−443.
40. Aiyar, J., Grissmer, S., and Chandy, K. G. (1993) Full-length and truncated Kv1.3 K^+ channels are modulated by 5-HT receptor activation and independently by PKC, *Am. J. Physiol. 265*, C1571−C1578.
41. Kobertz, W. R., and Miller, C. (1999) K^+ channels lacking the 'tetramerization' domain: implications for pore structure, *Nat. Struct. Biol. 6*, 1122−1125.
42. Zerangue, N., Jan, Y. N., and Jan, L. Y. (2000) An artificial tetramerization domain restores efficient assembly of functional *Shaker* channels lacking T1, *Proc. Natl. Acad. Sci. U.S.A. 97*, 3591−3595.
43. Tu, L., and Deutsch, C. (1999) Evidence for dimerization of dimers in K^+ channel assembly, *Biophys. J. 76*, 2004−2017.
44. Lu, J., Robinson, J. M., Edwards, D., and Deutsch, C. (2001) T1−T1 interactions occur in ER membranes while nascent Kv peptides are still attached to ribosomes, *Biochemistry 40*, 10934−10946.
45. Shoemaker, B. A., Portman, J. J., and Wolynes, P. G. (2000) Speeding molecular recognition by using the folding funnel: the fly-casting mechanism, *Proc. Natl. Acad. Sci. U.S.A. 97*, 8868−8873.
46. Robinson, J. M., and Deutsch, C. (2005) Coupled tertiary folding and oligomerization of the T1 domain of Kv channels, *Neuron 45*, 223−232.

BI700319F